Communication

Detection of a High-Barrier Conformational Change in the Active Site of Cytochrome P450 upon Binding of Putidaredoxin

Julie Y. Wei, Thomas C. Pochapsky, and Susan Sondej Pochapsky

J. Am. Chem. Soc., **2005**, 127 (19), 6974-6976• DOI: 10.1021/ja051195j • Publication Date (Web): 23 April 2005

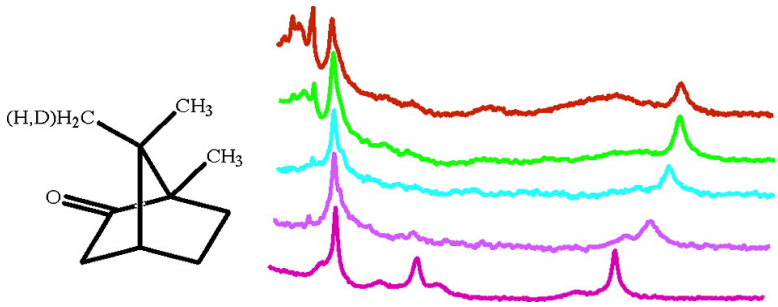

J|A|C|S
COMMUNICATIONS

Published on Web 04/23/2005

Detection of a High-Barrier Conformational Change in the Active Site of Cytochrome P450$_{cam}$ upon Binding of Putidaredoxin

Julie Y. Wei, Thomas C. Pochapsky,* and Susan Sondej Pochapsky

Department of Chemistry, Brandeis University, 415 South Street MS 015, Waltham, Massachusetts 02454-9110

Received February 24, 2005; E-mail: pochapsk@brandeis.edu

Cytochrome P450$_{cam}$ (CYP101) catalyzes the 5-*exo*-hydroxylation of camphor **1**, the first step of catabolism of **1** by the soil bacterium *Pseudomonas putida*.[1] Two electrons are required for turnover, and the second reduction, of the Fe(II) P450$_{cam}$−O_2−**1** ternary complex (CYP−**1**−O_2), is the rate-limiting step under physiological conditions.[2] The presence of an effector is required for the formation of hydroxycamphor product.[3] The Fe_2S_2 ferredoxin putidaredoxin (Pdx) is the biological effector and reductant of CYP101.[3] Structural perturbations have been observed spectroscopically in the CYP101 active site upon binding of Pdx, and it has been proposed that these perturbations are involved in the effector and/or electron-transfer activity of Pdx.[4−9]

The complex between reduced Pdx (Pdx^r) and reduced **1**- and CO-bound P450$_{cam}$ (CYP−**1**−CO) is often used as a model for the catalytically competent Pdx^r−CYP−**1**−O_2 complex and is convenient for NMR spectroscopy in that the heme is diamagnetic. Recently, we reported perturbations in the conformational equilibrium of CYP−**1**−CO as a function of addition of Pdx^r.[7] These perturbations were monitored by ^{1}H,^{15}N HSQC experiments using sequence-specific resonance assignments in CYP101. In addition to changes that take place in the proposed interface between the two proteins, we identified perturbations in regions of the P450$_{cam}$ molecule that have been shown to be involved in substrate access and orientation, including the B′, F, and G helices and portions of the β3 sheet. On this basis, we proposed a dynamic model for the effector activity of Pdx, in which binding of Pdx forces selection of the active conformation of CYP101 from a manifold of conformations, and we suggested that the conformational changes observed in the substrate access region are critical to this selection. The conformation thus selected prevents loss of substrate and/or intermediates and enforces the correct orientation of the substrate with respect to the activated oxygen. In other work, Tosha et al. reported perturbations in the ^{1}H NMR spectrum of CYP−**1**−CO as a function of Pdx^r addition that indicate changes in the orientations of **1**, the active site Thr252, and the distal Fe ligand cysteine thiolate CH_2 group in the presence of Pdx^r.[6] Here, we present evidence for a high-barrier conformational shift in CYP−**1**−CO upon binding of Pdx^r that results in changes in the environment of camphor in the active site.

Highly perdeuterated C334A CYP101 was expressed, purified, reduced, and prepared for NMR spectroscopy in D_2O buffer as described previously.[7] The C334A mutant of CYP101 has been shown to be spectroscopically and enzymatically identical to wild-type enzyme, but does not form dimers in solution.[10] Perdeuterated Pdx was expressed in a manner similar to that of CYP101, reconstituted, and purified, according to the method of Jain,[11] and was then reduced with sodium dithionite for titration as described previously.[7] 8-d_1-**1** was synthesized by the method of Dadson et al.[12,13] NMR spectroscopy was performed on a Varian INOVA 600 MHz NMR spectrometer. All ^{1}H and ^{13}C chemical shifts are reported in parts per million relative to TSP (trimethylsilylpropionic acid sodium salt).

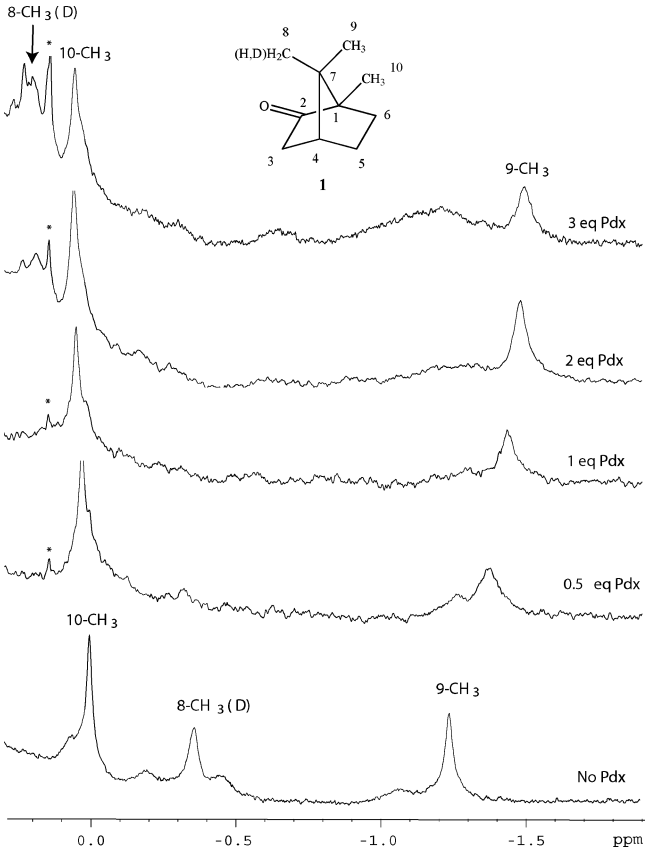

Figure 1. Series of ^{1}H NMR spectra showing titration of perdeuterated CYP101−**1**−CO at 14 T (600 MHz ^{1}H) with perdeuterated Pdx^r. Starting concentration of CYP101 is 0.3 mM. Both proteins were dissolved in 2 mM 8-d_1-camphor **1**, 100% D_2O, pH 7.4 phosphate buffer (uncorrected for isotope effects), 298 K, with perdeuterated Pdx^r. The signals observed are primarily those of CYP-bound 8-d_1-**1**. Note that the integration of the 8-CH_3 signal is less than that of the other two methyl groups due to the presence of a single deuterium at that position, and the peak is also shifted slightly upfield from the position observed with all protio-**1** (data not shown) due to an isotope shift. Peak marked with an asterisk is an exchangeable proton observed in CYP101 when H_2O is present. The inset shows the structure of camphor **1** with carbon atom numbering.

Three methyl signals are observed in the upfield region of the ^{1}H spectrum of perdeuterated CYP−**1**−CO that were assigned from ^{1}H,^{13}C HSQC data to the 10-CH_3, 8-CH_3, and 9-CH_3 resonances of CYP101-bound **1**. The assignment of the 10-CH_3 is based on the distinctive upfield ^{13}C shift of that resonance.[14] The assignment of the 8-CH_3 was confirmed by the attenuation and isotope shift of that signal when 8-d_1-**1** is used to prepare the CYP101 sample (Figure 1). The 9-CH_3 ^{1}H assignment is by elimination and agrees with that of Tosha et al.[6] Using the published structure of CO-

10.1021/ja051195j CCC: $30.25

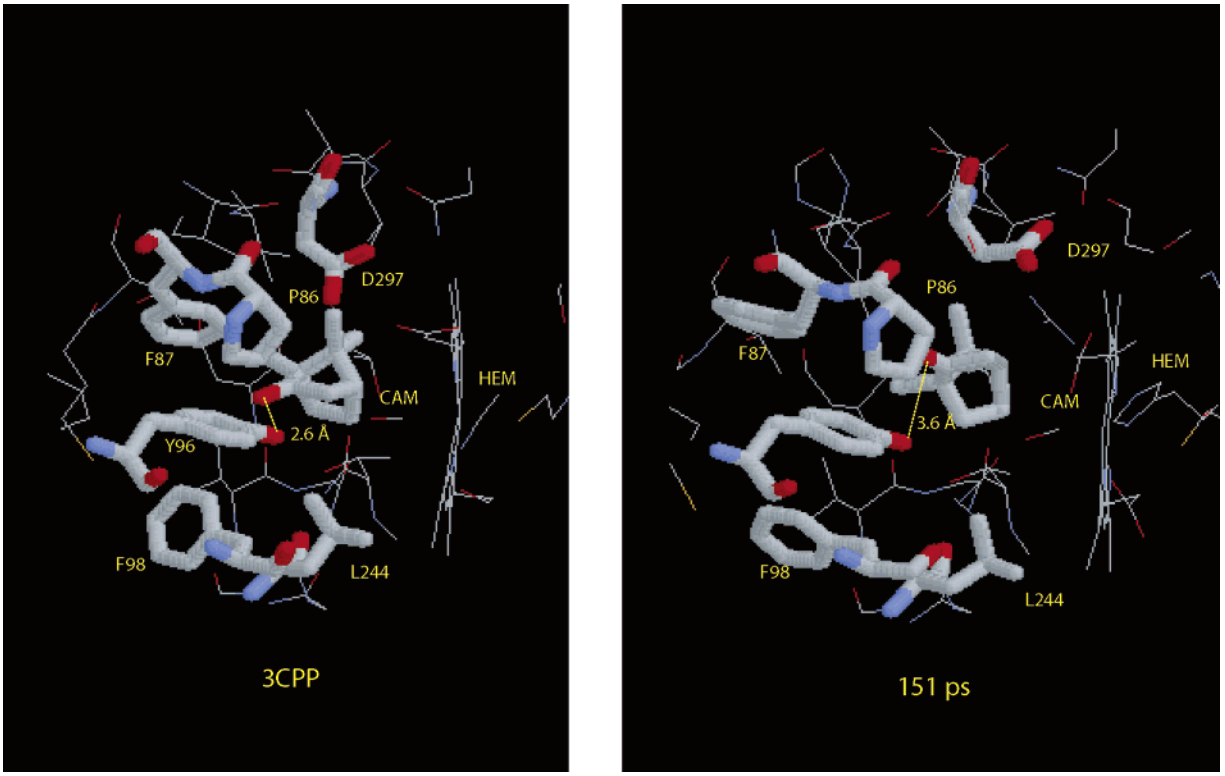

Figure 2. Comparison of CYP101 active site from PDB structure 3CPP (ref 15) (left) and the structure identified after 151 ps of restrained molecular dynamics simulation that minimizes ring current shift violations (right). See text for details.

bound CYP101 (PDB entry 3CPP),[15] ring current shifts expected to bind **1** due to the heme porphyrin ring and nearby aromatic residues were calculated using SHIFTS (D. Case, Scripps Research Institute, La Jolla, CA).[16] The agreement between observed and calculated ^{1}H shifts is within error limits ($\Delta\delta = \pm 0.3$) for the 10-CH_3 ($\Delta\delta_H = -0.20$) and the 9-CH_3 ($\Delta\delta_H = -0.16$). However, the ^{1}H signal of the 8-CH_3 group of **1** is shifted well upfield of predicted values ($\Delta\delta_H = -0.80$), indicating that this methyl group is experiencing considerably more ring current shift than is predicted from the 3CPP structure (Figure 1, bottom, and Table 1).

Using the experimental ring current shifts for the methyl groups of **1** in the absence of Pdx as an energetic constraint, we performed a 170 ps vacuum molecular dynamics simulation at 300 K in order to sample conformations of the CYP101 active site and orientations of **1** that could give rise to the chemical shifts observed in the absence of Pdx. The 3CPP crystal structure with hydrogens added, but without external waters, was used as a starting point for the simulation. Initially, the structure relaxed to a manifold of states (average root mean square deviation (RMSD) = 2 Å), where it remained until 80 ps had elapsed. In this manifold, the ring current shifts' constraints showed an average total violation for the three methyls of **1** $|\Delta\delta| = 1.41$. After 80 ps, a transition takes place over 30 ps into a manifold of states that persists until the end of the simulation. This manifold has a higher overall RMSD (average RMSD = 2.5 Å) than that in the earlier simulation and gives a lower average ring current shift violation ($|\Delta\delta| = 1.02$). The transition between 80 and 110 ps is correlated with (and apparently driven by) the lowering of the total ring current shift violation. The structure with the lowest total ring current shift violations (at 151 ps, $|\Delta\delta| = 0.56$) was selected for examination. The most obvious difference between that structure and 3CPP is a ~20° rotation of **1** around a vector between atoms C1 and C5 (Figure 2). The rotation does not displace the 10-CH_3 significantly, relative to the heme, but moves the 8-CH_3 into a position more directly over the heme ring. The 9-CH_3 remains at about the same distance from the heme as in 3CPP but is slightly closer to the heme normal. The rotation increases the distance between the carbonyl oxygen of **1** and the hydroxyl group of Tyr96 out of hydrogen bonding range. There are fewer van der Waals contacts between distal residues and the 8-CH_3 in the ring current driven structure, and the side chains of Phe87 and Asp297 are both visibly displaced to accommodate the new orientation of **1**. These changes represent an expansion of the distal binding pocket in order to accommodate the ring current shift driven orientation (Figure 2).

Table 1. ^{1}H Chemical Shifts of CYP−**1**−CO-Bound **1** Methyls as a Function of Pdx^r Binding (298 K)[a]

methyl	^{13}C δ_{obs}	^{1}H δ_{calcd}	^{1}H δ_{obs}, no Pdx	^{1}H δ_{obs} + 3 equiv of Pdx^r
8-CH_3	21.1	0.51	−0.33 (−0.84)	0.20 (−0.31)
9-CH_3	18.8	−1.38	−1.22 (+0.16)	−1.48 (−0.08)
10-CH_3	10.4	0.22	0.02 (−0.20)	0.06 (−0.04)

[a] Calculated shifts are obtained using the SHIFTS program[14] with PDB entry 3CPP. The difference between observed and calculated shifts ($\delta_{calcd} - \delta_{obs}$) are shown in parentheses next to δ_{obs}.

Titration of samples of perdeuterated CYP−**1**−CO in D_2O with perdeuterated Pdx^r allowed us to observe perturbations to camphor ^{1}H signals resulting from the formation of the Pdx^r−CYP−**1**−CO complex without interference from protein ^{1}H signals. Titration curves derived from chemical shift perturbations were consistent with the K_d for the Pdx^r−CYP−**1**−CO complex measured previously by our group[7] and Tosha et al.,[6] indicating that the same event is being monitored. Of the three camphor methyl signals, the most dramatic response to the presence of Pdx^r is observed at the 8-CH_3 resonance, which undergoes an exchange phenomenon that is slow on the chemical shift time scale at 298 K and 14 T magnetic field. The 8-CH_3 resonance does not shift, but broadens drastically, and is essentially undetectable after 0.5 equiv of Pdx^r has been added (Figure 1). At saturating Pdx concentrations, a new resonance at $\delta = 0.20$ ppm appears that gives rise to an NOE cross-

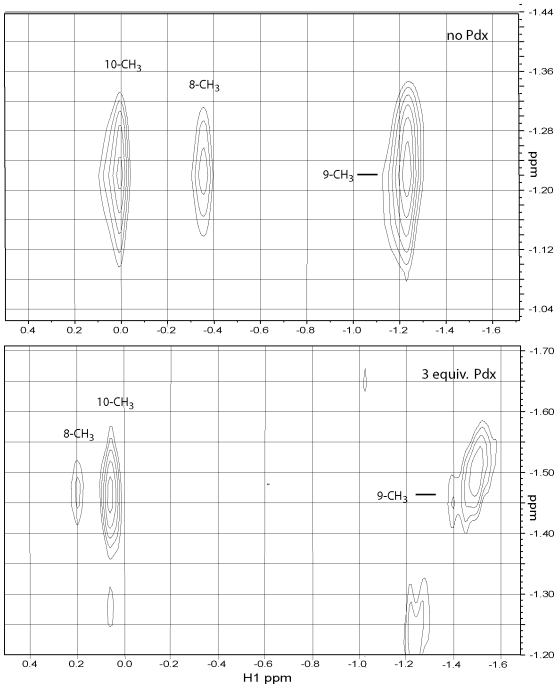

Figure 3. Region of 600 MHz ^{1}H NOESY spectra (t_{mix} = 500 ms) showing cross-peaks between 9-CH_3 of **1** (vertical axes) and the 8- and 10-CH_3 groups of **1** bound to perdeuterated CYP101−CO: (top spectrum) no Pdx^r; (bottom spectrum) 3 equiv of perdeuterated Pdx^r. Sample conditions are the same as that in Figure 1. The signal intensity at the 8-CH_3 is attenuated by deuteration.

peak to the 9-CH_3 resonance (Figure 3). The identity of this resonance as 8-CH_3 was confirmed using 8-d_1-camphor. From the difference in chemical shift between the two resonances assigned to the 8-CH_3, the exchange rate must be no greater than 300 s^{-1} at 298 K. The shift change of the 9-CH_3 signal (which is at fast exchange) gives a lower limit of 150 s^{-1}.

For the 10-CH_3 ^{1}H resonance, only a small difference is seen between the chemical shift in the absence of Pdx and when Pdx is saturating ($\Delta\delta_{max} = +0.05$). The line width of the 10-CH_3 remains essentially constant throughout the titration. As reported by Tosha et al.,[6] the 9-CH_3 ^{1}H resonance showed a somewhat larger chemical shift change ($\Delta\delta_{max} = -0.24$) from 0 to 3 equiv of Pdx with noticeable broadening near the midpoint of the titration. It is interesting that the chemical shifts observed for the methyl groups of **1** at saturating Pdx concentrations are in better agreement with those predicted from the 3CPP structure than in the absence of Pdx (Table 1). This suggests to us that the crystallographic structure may better represent the active site conformation selected upon Pdx binding (that is, the enzymatically competent conformation) than the manifold of conformations present in solution in the absence of Pdx. This would also explain why X-ray-generated photoelectrons are capable of supporting hydroxylation of **1** in a CYP101 crystal in the absence of effector.[17]

The observation of a process at slow exchange on the chemical shift time scale in protein structure is often associated with cis-trans isomerization of a X−Pro peptide linkage.[18] We note that Pro86 is in proximity to bound **1** in the active site and is structurally and spatially adjacent to many of the residues that we observed previously to be affected by the addition of Pdx, including residues in the B′ helix and the β3 sheet. Although the Cys85−Pro86 peptide bond is in the all-trans conformation in 3CPP, the possibility that it or other proline residues might be capable of cis-trans isomerization in solution should not be discounted. We are currently testing this hypothesis experimentally.

Acknowledgment. This work was supported in part by grants from the U.S. National Institutes of Health, R01-GM44191 and R01-GM067786 (T.C.P.)

Supporting Information Available: Input files for AMBER, selected dynamics traces, and supporting NMR information. This material is available free of charge via the Internet at http://pubs.acs.org.

References

(1) Mueller, E. J.; Loida, P. J.; Sligar, S. G. In *Cytochrome P450: Structure, Function and Biochemistry*, 2nd ed.; Ortiz de Montellano, P., Ed.; Plenum Press: New York, 1995; pp 83−124.
(2) Brewer, C. B.; Peterson, J. A. *J. Biol. Chem.* **1988**, *263*, 791−798.
(3) Lipscomb, J. D.; Sligar, S. G.; Namtvedt, M. J.; Gunsalus, I. C. *J. Biol. Chem.* **1976**, *251*, 1116−1124.
(4) Unno, M.; Christian, J. F.; Sjodin, T.; Benson, D. E.; Macdonald, I. D. G.; Sligar, S. G.; Champion, P. M. *J. Biol. Chem.* **2002**, *277*, 2547−2553.
(5) Sjodin, T.; Christian, J. F.; Macdonald, I. D. G.; Davydov, R.; Unno, M.; Sligar, S. C.; Hoffman, B. M.; Champion, P. M. *Biochemistry* **2001**, *40*, 6852−6859.
(6) Tosha, T.; Yoshioka, S.; Takahashi, S.; Ishimori, K.; Shimada, H.; Morishima, I. *J. Biol. Chem.* **2003**, *278*, 39809−39821.
(7) Pochapsky, S. S.; Pochapsky, T. C.; Wei, J. W. *Biochemistry* **2003**, *42*, 5649−5656.
(8) Nagano, S.; Tosha, T.; Ishimori, K.; Morishima, I.; Poulos, T. L. *J. Biol. Chem.* **2004**, *279*, 42844−42849.
(9) Tosha, T.; Yoshioka, S.; Ishimori, K.; Morishima, I. *J. Biol. Chem.* **2004**, *279*, 42836−42843.
(10) Nickerson, D. P.; Wong, L. L. *Protein Eng.* **1997**, *10*, 1357−1361.
(11) Jain, N. U.; Pochapsky, T. C. *Biochem. Biophys. Res. Commun.* **1999**, *258*, 54−59.
(12) Dadson, W. M.; Money, T. *J. Chem. Soc., Chem. Commun.* **1982**, 112−113.
(13) Dadson, W. M.; Hutchinson, J. H.; Money, T. *Can. J. Chem.* **1990**, *68*, 1821−1828.
(14) Crull, G. B.; Garber, A. R.; Kennington, J. W.; Prosser, C. M.; Stone, P. W.; Fant, J. W.; Dawson, J. H. *Magn. Reson. Chem.* **1986**, *24*, 737−739.
(15) Raag, R.; Poulos, T. L. *Biochemistry* **1989**, *28*, 7586−7592.
(16) Case, D. A. *J. Biomol. NMR* **1995**, *6*, 341−346.
(17) Schlichting, I.; Berendzen, J.; Chu, K.; Stock, A. M.; Maves, S. A.; Benson, D. E.; Sweet, B. M.; Ringe, D.; Petsko, G. A.; Sligar, S. G. *Science* **2000**, *287*, 1615−1622.
(18) Bosco, D. A.; Eisenmesser, E. Z.; Pochapsky, S.; Sundquist, W. I.; Kern, D. *Proc. Natl. Acad. Sci. U.S.A.* **2002**, *99*, 5247−5252.

JA051195J